SSRG International Journal of Electrical and Electronics Engineering
ISSN: 2348-8379/ https://doi.org/10.14445/23488379/IJEEE-V11I11P135

Volume 11 Issue 11, 373-380, November 2024

Original Article

Fuzzy Based VSG Control Technique for Dynamic Frequency Regulation Enhancement in AC Microgrid

S. Nivedha[1], P. Lakshmi[2], P. Somasundaram[3]

[1,2,3]*Department of Electrical and Electronics Engineering, College of Engineering Guindy, Chennai, India*

[1]*Corresponding Author : 2019209003@student.annauniv.edu*

Received: 20 September 2024 Revised: 21 October 2024 Accepted: 19 November 2024 Published: 30 November 2024

Abstract *- Voltage Source Converter (VSC) interfaced with Distributed Generators (DG's) in microgrids possess rapid frequency fluctuations in the event of disturbances due to lack of inertia. The Virtual Synchronous Generator (VSG) technique is employed to control the inverter and mimic the inertia characteristic of the synchronous generator. The VSG technique's Power-frequency (P-f) droop regulates frequency within permissible limits. The proportional controller is used to provide primary frequency control in P-f droop. To maintain the frequency at the nominal value when subjected to disturbances, frequency regulation is further enhanced by a secondary frequency controller. The integral controller is combined with the proportional controller in P-f droop to regulate the frequency at a nominal value. However, the PI controller in P-f droop regulates frequency slower, and the frequency oscillates in the event of disturbances. The dynamic frequency regulation can be enhanced with the fuzzy PI controller by regulating the frequency deviation faster at the nominal value. The improved dynamic frequency regulation maintains the frequency nadir of the microgrid and restores faster when subjected to disturbances. The fuzzy logic is introduced to enhance the dynamic frequency regulation in the proposed Fuzzy based VSG control technique. The adaptive variation of the PI controller gains with the Fuzzy Logic Controller (FLC) in the event of disturbances such as changes in load and mode of operation of DG, raising the frequency stability of DG. The performance of the proposed control technique is validated with simulations in MATLAB/Simulink.*

Keywords *- Dynamic frequency regulation, Fuzzy Logic Controller, Inverter, Microgrid, Virtual Synchronous Generator.*

1. Introduction

Inverter Based Resources (IBR) increased in power systems in the past decade. The emission-free energy provided by Renewable Energy Source (RES) motivates the integration of IBR into the power grid [1]. The microgrid has an inverter controlled by P-Q and V-f techniques, allowing DG to operate in grid-forming or grid-following modes [2]. The inverters interfaced with RES possess no inertia. This causes various issues in the power system, such as reduced small signal and large signal stability and voltage and frequency instability [3]. The Virtual Synchronous Generator (VSG) technique is implemented in the inverter to emulate inertia similarly to a synchronous generator [4].

The P-f droop in the VSG control technique regulates the frequency and provides mechanical power reference to the active power loop. The Q-V droop functions to provide a reference voltage to the voltage controller. In a conventional VSG control structure, the frequency deviates from the nominal value in the event of disturbances such as load variations and changes in the mode of operation of DG. This causes undesirable frequency oscillations away from the nominal value [4, 5].

To enhance the frequency regulation and dynamic performance of VSG, the cooperative control of inertia and damping is implemented in the active power loop of the VSG control technique [6]. In [7], adaptive virtual inertia control is implemented to increase frequency stability with a bang-bang control strategy. In [8], adaptive control of inertia improves the frequency regulation of microgrids in a system with multiple inverters connected in parallel. However, no analysis on reducing the response time is provided.

In [9], neural network-based integral sliding mode backstepping control is proposed to improve the dynamic performance of VSG in grid-connected inverters by controlling measurement disturbances and errors. In [10], the Adaptive Neuro Fuzzy Inference System (ANFIS) controller controls the mechanical reference power input of VSG and the dynamic frequency stability is enhanced. However, the computational complexity of the controller is high. In [11], a fuzzy controller is employed to provide reference power in the active power loop of VSG in a grid-connected inverter, enhancing the dynamic performance. However, this control is applicable only when multiple inverters are connected in parallel.

In [12], the adaptive inertia control is modelled to enhance the frequency regulation of the inverter controlled by the VSG technique in the microgrid. However, the influence of the damping factor in frequency response is not considered. In [13], cascaded Model Predictive Control (MPC) is introduced in the VSG control loop to reduce frequency error in load-switching cases of islanded microgrids. However, it requires derivative control action to increase the complexity of control.

In [14], the synchronization of microgrids in various operating modes is improved by adding a frequency compensation link. However, the hardware complexity is high in the control loop. The improvement in frequency response by control of inertia constant in VSG controller is widely focused, but inertia also influences voltage stability and power oscillation in the system. Therefore, power frequency droop can be focused to improve the frequency regulation of the system.

In [15], the optimal damping coefficient is used in the event of a change in the operating mode of the microgrid. The frequency regulation is improved by combining the integral controller together with a proportional controller in P-f droop. In the event of disturbances, the P-f droop provides frequency deviation, and the PI controller in the P-f droop takes time to settle the frequency at a nominal value. To enhance the dynamic frequency regulation, the P-f droop is incorporated with a Fuzzy Logic Controller (FLC) to tune the PI controller to dampen the frequency oscillation. The mechanical power reference is provided by P-f droop. The enhanced mechanical power input reference minimizes the frequency deviation and provides phase angle reference to the inverter.

This paper proposes a novel control strategy for enhancing dynamic frequency regulation by incorporating the power frequency droop with the fuzzy PI controller. The performance of a fuzzy-based VSG controller is compared with that of a conventional PI controller [15]. The proposed work is presented in the rest of the sections as follows. Section 2 consists of modeling VSG, P-f droop with PI controller and fuzzy PI controller for frequency regulation in VSG control strategy. Section 3 describes the simulation results, and Section 4 describes the conclusion.

2. VSG Control Structure

2.1. Microgrid Structure

The microgrid integrates Renewable Energy Sources (RES) such as PV units, wind turbines, hydro energy, biomass, etc., known as Distributed Generator (DG), energy storage units and inverters connected to the load. In Figure 1, the AC microgrid, RES, and energy storage devices act as the input energy source to the inverter to supply the load in the microgrid and utility grid [16-18].

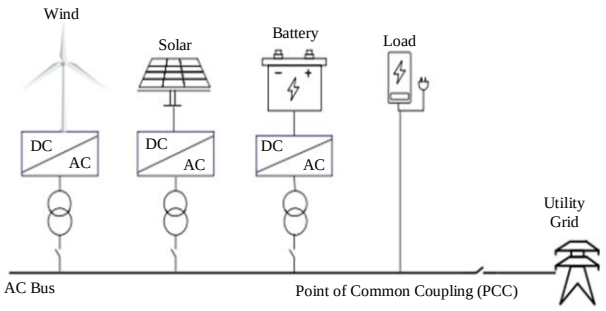

Fig. 1 Structure of microgrid

2.2. VSG Control Strategy

The DG in microgrids does not inherently possess inertia similar to traditional grids. This causes frequency instability in the microgrid in the event of disturbances. The inverter connected to the DGs is controlled to mitigate the frequency instability. The Virtual Synchronous Generator (VSG) inverter technique mimics the inertia characteristic of traditional Synchronous Generator (SG). The DG interfaced with the inverter in the microgrid is considered for implementing the VSG inverter control technique, as shown in Figure 2.

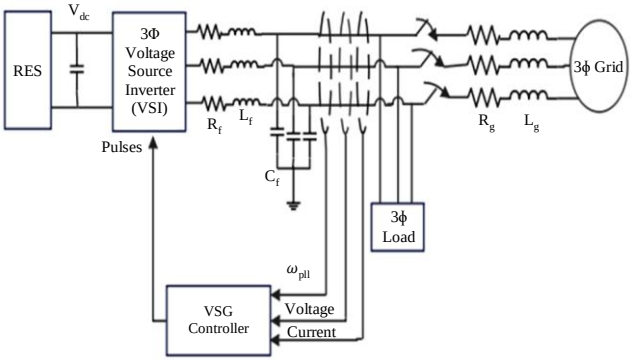

Fig. 2 Structure of DG with VSG control technique

The output of the inverter is filtered by inductance L_f and capacitance C_f, which are connected to the load and utility grid. The VSG control structure has two outer control loops and three inner control loops. The P-f droop and Q-V droop reference the inner control loop. The active power loop, voltage controller, and current controller work as an inner control loop. The Q-V droop provides reference voltage with a slower response to the inner loop. The P-f droop provides frequency regulation and maintains the frequency within allowable limits in the event of disturbances. The P-f droop consists of a primary and secondary frequency controller to minimize frequency deviation.

The primary and secondary frequency control is described by the Equation (1) and (2) as follows,

$$P_m = P_{ref} + K_p(\omega_o - \omega_{pll}) \quad (1)$$

$$P_m = P_{ref} + \left(\frac{K_i}{s}\right)(\omega_o - \omega_{pll}) \quad (2)$$

In Equations (1) and (2), P_m is the mechanical power, P_{ref} is the reference power, ω_o is the rated angular frequency, ω_{pll} is the instantaneous angular frequency in rad/s measured at inverter output, K_p and K_i are of PI controller gains in P-f droop.

The secondary frequency control combined with primary frequency control in P-f droop is given in Equation (3). The P-f droop structure with primary and secondary frequency control is shown in Figure 3 [12].

$$P_m = P_{ref} + \left(K_p + \frac{K_i}{s}\right)(\omega_o - \omega_{pll}) \quad (3)$$

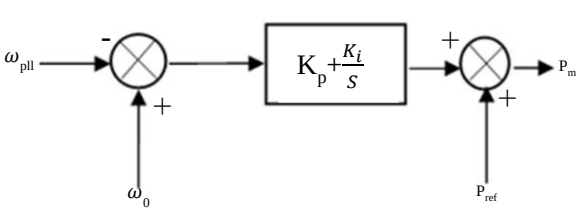

Fig. 3 Structure of P-f droop

The power-frequency droop provides input mechanical power reference. The active power loop has a swing equation that functions to provide a reference phase angle to control the inverter. The inertia and damping coefficient in an active power loop also influence the frequency regulation of the inverter. The damping coefficient of VSG is kept at an optimal value of 38 in islanded mode and 238 in grid-connected mode to ensure improved performance in the system [12].

The VSG technique is implemented to control the inverter. The active and reactive power loop equations of VSG are described in (4) and (5) as follows: [13-15]

$$T_m - T_e - T_d = J\frac{d\omega_{pll}}{dt} \quad (4)$$

$$E = U_o + \frac{1}{D_q}(Q_{ref} - Q_e) \quad (5)$$

In Equation (4) and (5), T_m is the mechanical torque, T_e is the electrical torque, T_d is the damping torque, J is the inertia coefficient, E is the reference voltage, U_o is the instantaneous output voltage, D_q is the reactive power droop coefficient, Q_{ref} is the reference reactive power, Q_e is the instantaneous reactive power output.

The Q-V droop provides voltage reference to the voltage controller. The voltage controller maintains the inverter's output voltage to its reference voltage provided by the Q-V droop by the PI controller [16, 17]. The PI controller is tuned using the Ziegler-Nichols tuning method. The voltage controller provides reference input current to the current controller, and Equation describes it (6) and (7),

$$i^*_{m,d} = \left(K_{pv} + \frac{K_{iv}}{s}\right)(v^*_d - v_d) - C_f\omega_{pll}v_q \quad (6)$$

$$i^*_{m,q} = \left(K_{pv} + \frac{K_{iv}}{s}\right)(v^*_q - v_q) + C_f\omega_{pll}v_d \quad (7)$$

The current controller functions to regulate current to its reference provided by the voltage controller through PI controllers [18]. It provides a reference voltage to control the inverter, and it is described by the Equations (8) and (9),

$$u_d = v_d - L_f\omega_{pll}i_{m,q} + (K_{pi} + \frac{K_{ii}}{s})(i^*_{m,d} - i_{m,d}) \quad (8)$$

$$u_q = v_q - L_f\omega_{pll}i_{m,d} + (K_{pi} + \frac{K_{ii}}{s})(i^*_{m,q} - i_{m,q}) \quad (9)$$

The reference voltage is provided to the PWM generator. The PWM generator provides a gate pulse to switch IGBT's in VSI. The simulation parameters of the DG and VSG control structure are represented in Table 1.

Table 1. Simulation parameters of microgrid

Symbol	Value
V_{dc}	750V
U_o	400V
L_f	1.7mH
C_f	10μF
R_f	0.1Ω
ω_0	314.1592 rad/s
J	6 s
D	38
D_q	0.002V/VAR
L_g	5mH
R_g	0.16Ω

3. Design of Fuzzy Based Power-Frequency Droop Control Technique

The PI controller in the P-f droop provides the frequency regulation. A fuzzy PI controller is implemented in P-f droop to enhance the dynamic frequency regulation of this proposed work. The control structure of fuzzy-based VSG is described in Figure 4. The Fuzzy PI controller functions to vary Kp and Ki outputs according to input variations through predefined rules. The structure of the fuzzy PI controller used for droop control is shown in Figure 5. The inputs to the Fuzzy Logic Controller (FLC) are error in frequency ($\Delta\omega$) and rate of change of error in frequency ($\frac{d\Delta\omega}{dt}$).

The output of FLC is K_p and K_i. The inputs are scaled by scaling factors. The input fuzzy variables are given as inputs to the mamdani Fuzzy Inference System (FIS), which consists of a rule base.

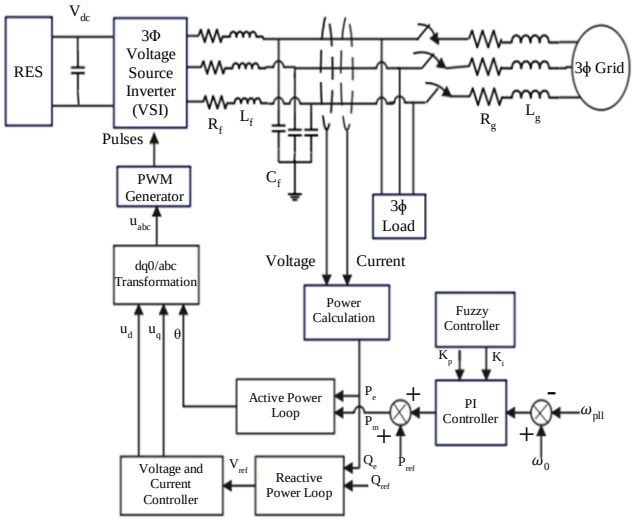

Fig. 4 VSG control structure

The input error in angular frequency (Δω) and rate of change of error angular frequency ($\frac{d\Delta\omega}{dt}$) are described in Equations (10) and (11),

$$\Delta\omega = \omega_o - \omega \tag{10}$$

$$\frac{d\Delta\omega}{dt} = \frac{\Delta\omega(k) - \Delta\omega(k-1)}{T} \tag{11}$$

In Equations (10) and (11), ω is the instantaneous inverter output frequency, and T is the sampling time.

The inputs of FLC are mapped to the output K_p and K_i in accordance with predefined rules. The rule table of K_p and K_i is shown in Table 2. The rules are defined by trial and error method. A triangular membership function is used to define the inputs and outputs.

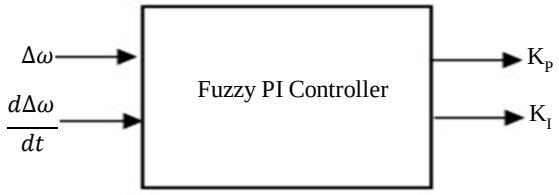

Fig. 5 Structure of proposed fuzzy PI controller for P-f droop

The inputs of FLC are divided into 5 membership functions: negative small NS, negative big NB, zero Z, positive big PB, and positive small PS. The output K_p and K_i are divided into 5 membership functions: Moderate Big MB, Moderate small MS, zero Z, big B and small S. The outputs K_p and K_i are defined by the same rule table, but the range of values differ for the K_p and K_i.

Mamdani's fuzzy inference system is used to map input and output using fuzzy logic. The de-fuzzified values of K_p and K_i are provided as the output of the fuzzy logic controller. The inputs, outputs and the fuzzy surface relating the inputs and outputs with the rulebase are shown in Figure 6.

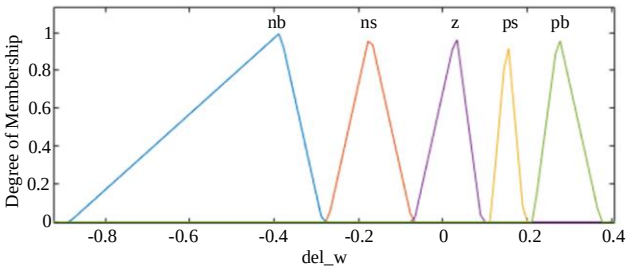

(a)

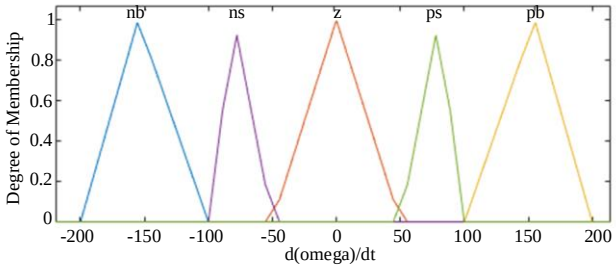

(b)

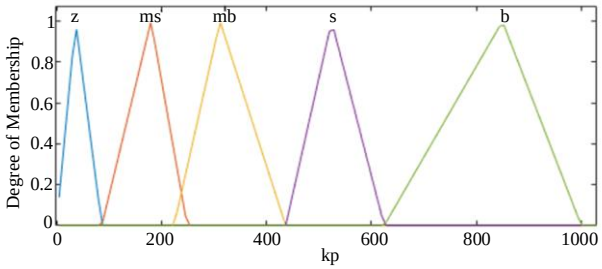

(c)

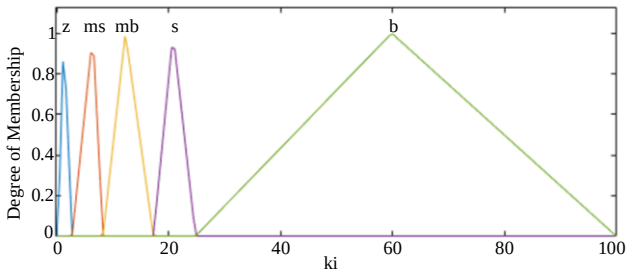

(d)

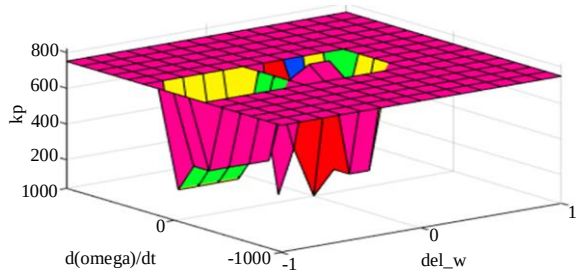

(e)

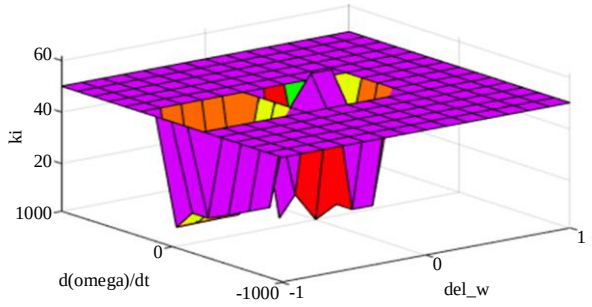

(f)

Fig. 6 Inputs and outputs of FLC (a) Δω, (b) $\frac{d\Delta\omega}{dt}$, (c) K_p, (d) K_i, (e) 3-D graph of rules defining K_p, and (f)3-D graph of rules defining K_i.

Table 2. Fuzzy rule table for K_p, K_i

Δ ω \ $\frac{d\Delta\omega}{dt}$	PB	PS	Z	NS	NB
PB	MB	MB	MS	MS	MS
PS	MB	MS	MS	Z	MS
Z	S	S	Z	B	B
NS	S	Z	MB	B	B
NB	MS	MS	MB	MB	MB

4. Results and Discussion

The RES is considered equivalent to the DC voltage source and is connected to the inverter, filter and load, as shown in Figure 6 [12, 13]. The inverter is controlled with the VSG control technique. The load consumed power is calculated by the line voltage and current at the inverter's Point of Common Coupling (PCC) connected to the load and utility grid.

The instantaneous output frequency is measured using Phase Locked Loop (PLL). At t=0, the inverter is operated in islanded mode, and the load power is 38 kW and 1.8kVAR, as observed in Figures 7(a) and 7(b). The nominal maximum value of phase voltage is 327 V, as observed in Figure 7(c). At the instant of switching from no load, the conventional PI controller in VSG provides a frequency deviation of 50.05Hz and settles at 50Hz in t=3s, as shown in Figure 7(d) after supplying the required load power. In the fuzzy PI controller, the proportional and integral coefficients are varied by the FLC in accordance with the predefined rules. This variation of K_p and K_i with FLC reduces the settling time of frequency deviation by 0.5 seconds.

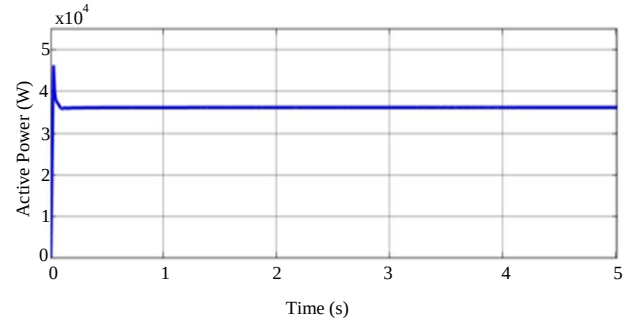

(a)

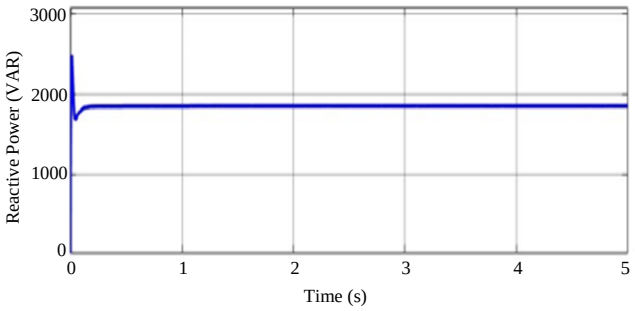

(b)

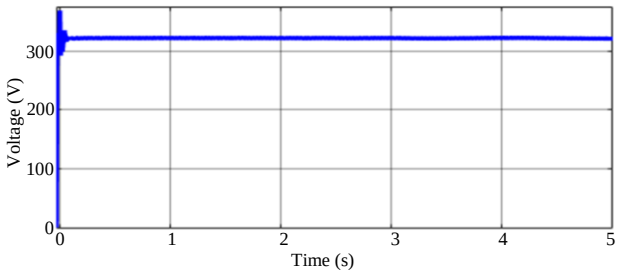

(c)

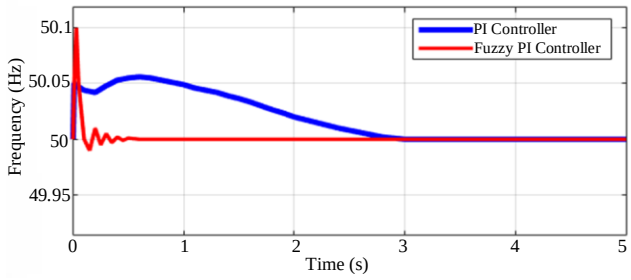

(d)

Fig. 7(a) Active power, (b) Reactive power, (c) Voltage, and (d) Frequency at the PCC with PI and fuzzy PI controller operating in islanded mode of operation.

At t=6s, the utility grid requires power, and the DG-connected inverter supplies power by operating in grid connected mode. The power the inverter supplies varies from 40kW and 2kVAR from 38kW and 1.8kVAR to supply the load, as observed in Figures 8 (a) and 8 (b). During the change in mode of operation, the PCC voltage is at 327V, as shown in Figure 8(c). The frequency deviation occurs for 2s with the PI controller at the instant of changing the mode of operation, as shown in Figure 8(d). The frequency deviation with fuzzy PI controller settles in 0.5s at the instant of changing the operating mode, maintaining the frequency nadir.

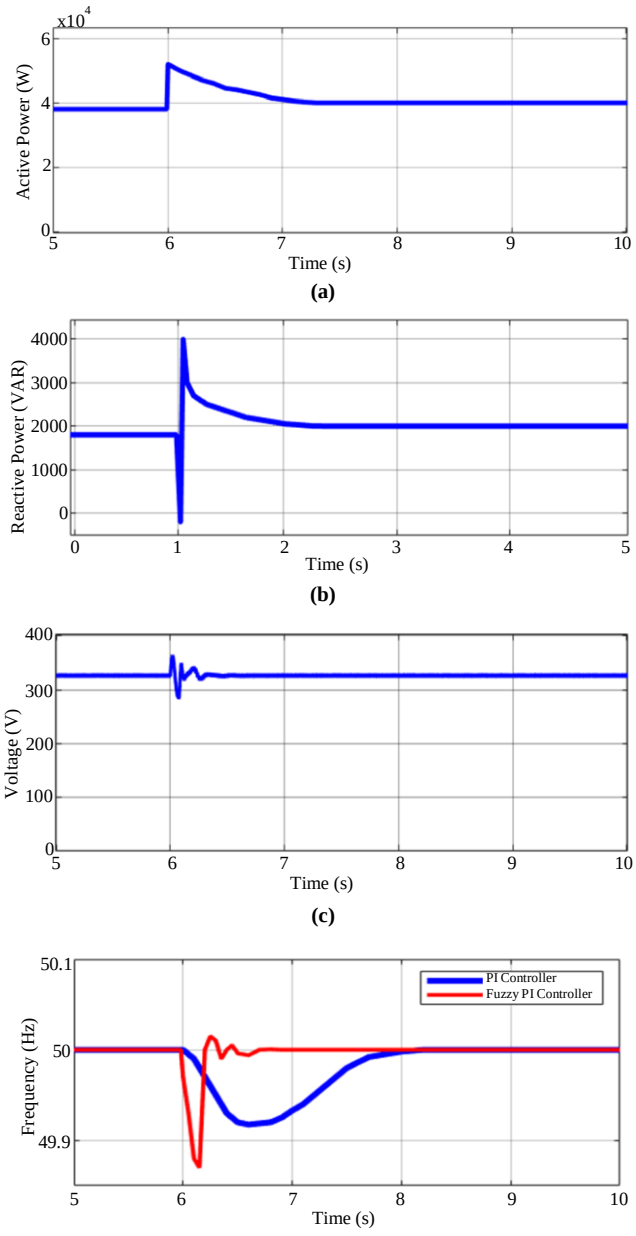

Fig. 8(a) Active power, (b) Reactive power, (c) Voltage, and (d) Frequency at the PCC with PI and fuzzy PI controller in the event of a change in mode of operation from islanded mode to grid-connected mode.

At t=10s, the inverter supplies the load in the microgrid, switches to islanded mode and disconnects from the grid. The power supplied by the inverter varies to 38kW and 1.8kVAR from 40kW and 2kVAR to supply the load in the grid, as observed in Figures 9(a) and 9(b). The PCC voltage during the transition in mode is at 327V with a transient during the transition, as shown in Figure 9(c). The frequency deviation occurs for 2s with the PI controller at the instant of changing from grid-connected mode to islanded mode, as shown in Figure 9(d). The frequency deviation with the fuzzy PI controller settles in 0.5s at the instant of changing the operating mode of an inverter.

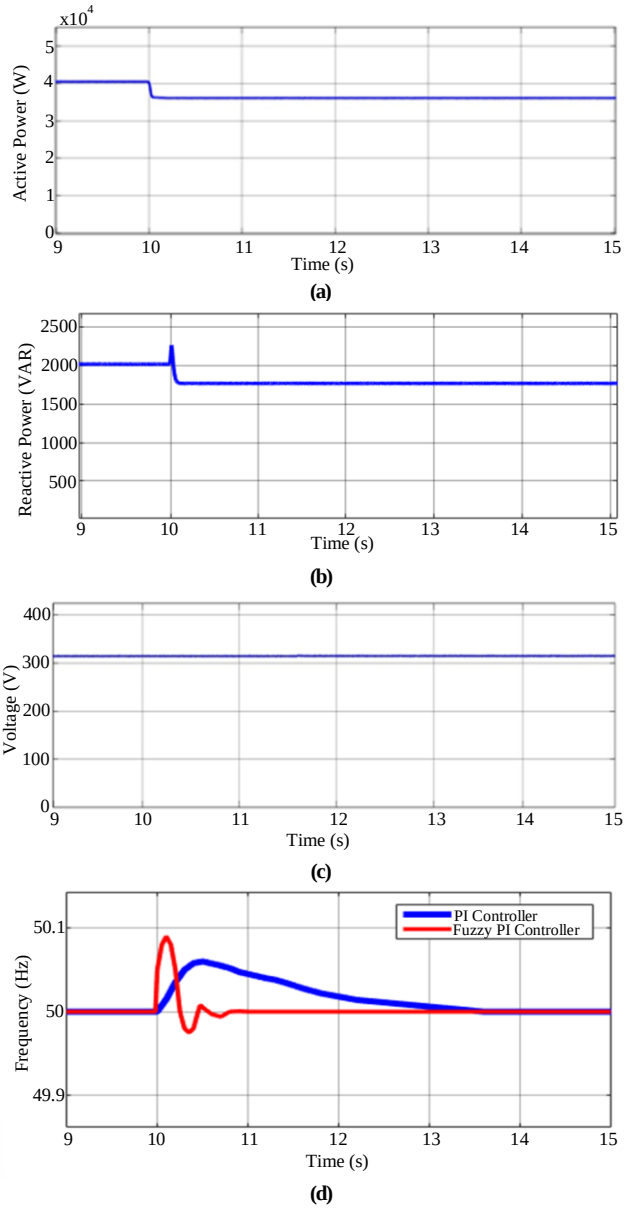

Fig. 9(a) Active power, (b) Reactive power, (c) Voltage, and (d) Frequency at PCC with PI and fuzzy PI controller in VSG in the event of a change in mode of operation from grid-connected mode to islanded mode.

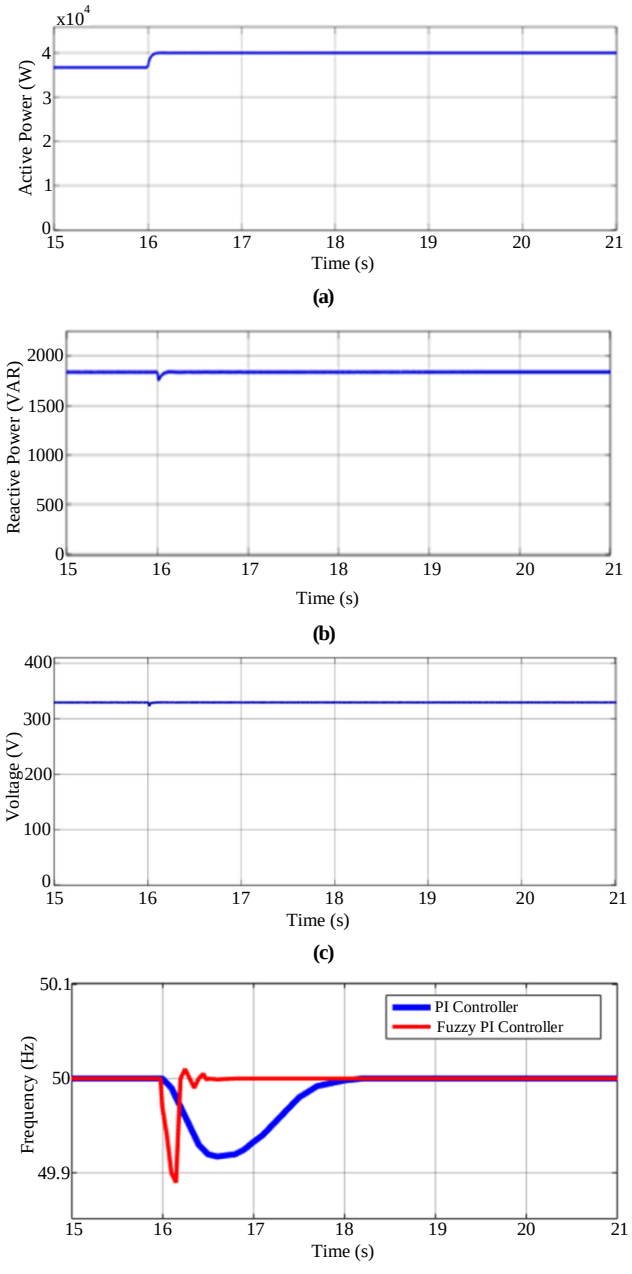

Fig. 10(a) Active power supplied by the inverter, (b) Reactive power supplied by the inverter, (c) Voltage at PCC, and (d) Frequency at PCC with PI and fuzzy PI controller in VSG in the event of load variations.

At t=16s, the load supplied by the inverter is increased from 38kW and 1.8kVAR to 40kW and 1.8kVAR, as shown in Figures 10(a) and 10(b). When load variations occur, the PCC voltage is at 327V with fluctuation, as observed in Figure 10(c). The conventional PI controller in P-f droop provides frequency deviation for 1.5 seconds in response in the event of load transition, as observed in Figure 10(d). The fuzzy PI controller reduces the frequency deviation in 0.5 seconds by adaptively varying the PI controller gains by FLC.

5. Conclusion

In this paper, dynamic frequency regulation is enhanced by adaptively changing the PI controller gains with FLC. The PI controller in P-f droop in VSG regulates frequency and reduces deviation in frequency in settling time of 2.8s in islanded mode, in 2s during transition to grid-connected mode from islanded mode, in 3s when operating mode changes to islanded mode from grid-connected mode and regulates frequency in settling time of 1.5s during load variations. The fuzzy PI controller in P-f droop minimizes frequency deviation and regulates frequency in a settling time of 0.5s in islanded mode and load variations and in a settling time of 0.6s during operating mode changes in microgrid. The frequency regulation with Fuzzy PI control is faster than the conventional PI controller in power-frequency droop.

The adaptive proportional and integral gains provided by the fuzzy PI controller minimize the frequency deviation instantaneously and improve the dynamic frequency regulation. The fuzzy PI controller provides enhanced dynamic frequency regulation compared to the conventional PI controller in P-f droop. The improved dynamic frequency regulation improves the frequency stability of the microgrid. The reduced overshoot in response, along with the reduced settling time, can effectively maintain the frequency nadir. The performance of the Fuzzy VSG technique shows reduced frequency settling time and enhanced dynamic frequency regulation compared to the conventional VSG technique.

Acknowledgments

The first author acknowledges and thanks the Centre for Research, Anna University, Chennai, for providing financial support through the AICTE Doctoral Fellowship (ADF) in carrying out this research.

References

[1] Yunjie Gu, and Timothy C. Green, "Power System Stability with a High Penetration of Inverter-Based Resources," *Proceedings of the IEEE*, vol.111, no. 7, pp. 832-853, 2023. [CrossRef] [Google Scholar] [Publisher Link]

[2] Amirhossein Sajadi et al., "Dynamics and Stability of Power Systems with High Shares of Grid-Following Inverter-Based Resources: A Tutorial," *IEEE Access*, vol. 11, pp. 29591-29613, 2023. [CrossRef] [Google Scholar] [Publisher Link]

[3] Haizhen Xu et al., "An Improved Virtual Inertia Algorithm of Virtual Synchronous Generator," *Journal of Modern Power Systems and Clean Energy*, vol. 8, no. 2, pp. 377-386, 2020. [CrossRef] [Google Scholar] [Publisher Link]

[4] Dayan B. Rathnayake, Reza Razzaghi, and Behrooz Bahrani, "Generalized Virtual Synchronous Generator Control Design for Renewable Power Systems," *IEEE Transactions of Sustainable Energy*, vol. 13, no. 2, pp. 1021-1036, 2022. [CrossRef] [Google Scholar] [Publisher Link]

[5] Fei Wang et al., "An Adaptive Control Strategy for Virtual Synchronous Generator," *IEEE Transaction of Industry Applications*, vol. 54, no. 5, pp. 5124-5133, 2018. [CrossRef] [Google Scholar] [Publisher Link]

[6] Shengwei Qu, and Zhijie Wang, "Cooperative Control Strategy of Virtual Synchronous Generator Based on Optimal Damping Ratio," *IEEE Access*, vol. 9, pp.709-719, 2020. [CrossRef] [Google Scholar] [Publisher Link]

[7] Jin Li, Buying Wen, and Taiyuan Wang, "Adaptive Virtual Inertia Control Strategy of VSG for Micro-Grid Based on Improved Bang-Bang Control Strategy," *IEEE Access*, vol. 7, pp. 39505-39514, 2019. [CrossRef] [Google Scholar] [Publisher Link]

[8] Amin Karimi et al., "Inertia Response Improvement in AC Microgrids: A Fuzzy-Based Control of Virtual Synchronous Generator," *IEEE Transactions on Power Electronics*, vol. 35, no. 4, pp. 4221-4331, 2020. [CrossRef] [Google Scholar] [Publisher Link]

[9] Qi Teng et al., "Neural Network-Based Integral Sliding Mode Backstepping Control for Virtual Synchronous Generators," *Energy Reports*, vol. 7, pp. 1-9, 2021. [CrossRef] [Google Scholar] [Publisher Link]

[10] Dina S.M. Osheba et al., "Performance Enhancement of PV System Using VSG with ANFIS Controller," *Electrical Engineering*, vol. 105, pp. 2523-2537, 2023. [CrossRef] [Google Scholar] [Publisher Link]

[11] Xiaochao Hou et al., "Improvement of Frequency Regulation in VSG-Based AC Microgrid via Adaptive Virtual Inertia," *IEEE Transaction of Power Electronics*, vol. 4, no. 3, pp. 1589-1602, 2020. [CrossRef] [Google Scholar] [Publisher Link]

[12] Rongliang Shi et al., "Self-Tuning Virtual Synchronous Generator Control for Improving Frequency Stability in Autonomous Photovoltaic-Diesel Microgrids," *Journal of Modern Power Systems and Clean Energy*, vol. 6, no. 3, pp. 482-494, 2018. [CrossRef] [Google Scholar] [Publisher Link]

[13] Tong Liu, "Double-Loop Control Strategy with Cascaded Model Predictive Control to Improve Frequency Regulation in Islanded Microgrids," *IEEE Transactions on Smart Grid*, vol. 13, no. 5, pp. 3954-3967, 2022. [CrossRef] [Google Scholar] [Publisher Link]

[14] Jianfeng Wang, Nurulazlina Ramli, and Noor Hafizah Abdul Aziz, "Pre-Synchronization Control Strategy of Virtual Synchronous Generator in Microgrid," *IEEE Access*, vol. 11, pp. 139004-139016, 2023. [CrossRef] [Google Scholar] [Publisher Link]

[15] Mobina Poursmaeil et al., "An Adaptive Parameter-Based Control Technique of Virtual Synchronous Generator for Smooth Transient between Islanded and Grid-Connected Mode of Operation," *IEEE Access*, vol. 9, pp. 137322-137337, 2021. [CrossRef] [Google Scholar] [Publisher Link]

[16] Ren Wang et al., "VSG-Based Adaptive Droop Control for Frequency and Active Power Regulation in the MTDC System," *CSEE Journal of Power and Energy Systems*, vol. 3, no. 3, pp. 260-268, 2017. [CrossRef] [Google Scholar] [Publisher Link]

[17] Meng Chen, Dao Zhou, and Frede Blaabjerg, "Modelling, Implementation, and Assessment of Virtual Synchronous Generator in Power Systems," *Journal of Modern Power Systems and Clean Energy*, vol. 8, no. 3, pp. 399-411, 2020. [CrossRef] [Google Scholar] [Publisher Link]

[18] Sepehr Saadatmand, Pourya Shamsi, and Mehdi Ferdowsi, "Power and Frequency Regulation of Synchronverters Using a Model Free Neural Network-Based Predictive Controller," vol. 68, no. 5, pp. 3662-3671, 2021. [CrossRef] [Google Scholar] [Publisher Link]